FIFTH-ORDER MOMENT CORRECTION FOR BEAM POSITION AND SECOND-ORDER MOMENT MEASUREMENT

K. Yanagida*, S. Suzuki, and H. Hanaki, JASRI, Sayo, Hyogo, Japan

Abstract

For the precise measurement of beam positions and second-order moments, we adopted a recursive correction with up to fifth-order moments for a measurement using a six-electrode BPM at SPring-8 linac. The higher-order correction terms are provided by considering an effect from higher-order moments on the output voltages of BPM. We found huge calculation error in a simulated correlation plot between set and calculated vertical positions without correction. This error is also found in a similar correlation plot between the measured vertical positions with fifth-order moment correction and without it.

INTRODUCTION

For measurements of beam position and second-order relative moments [1], six-electrode BPMs with circular cross-section have been installed at SPring-8 linac [2].

To obtain the relative attenuation factors between the BPM electrodes, we developed a beam-based calibration method, i.e., entire calibration. During the entire calibration, beams must be located at a position more than 4 mm from the BPM center.

We also developed a recursive correction scheme with up to fifth-order moments to improve the accuracy of the entire calibration when a beam was located far from the BPM center [3].

Previously, correction terms were usually expressed by the higher-order polynomials of the beam positions for obtaining (calculating) precise beam positions [4]. Because the correction terms came from higher-order moments that appeared on the output voltages of BPM, we constructed a new correction scheme whose correction terms were expressed by higher-order moments.

This paper describes the theoretical features of the correction scheme, the simulation (calculation) by an image charge method, and the experiment results using electron beams at SPring-8 linac.

THEORETICAL FEATURES

Electric Field Calculation

Figure 1 shows the structure of a six-electrode BPM with a circular cross-section that is used at SPring-8 linac. Inner radius R is 16 mm, and the shared radius of each electrode is $6/\pi$.

Suppose an M-particle system where b_N and β_N are the distance from the BPM center and an argument from the x-axis for Nth-charged particles (Fig. 1).

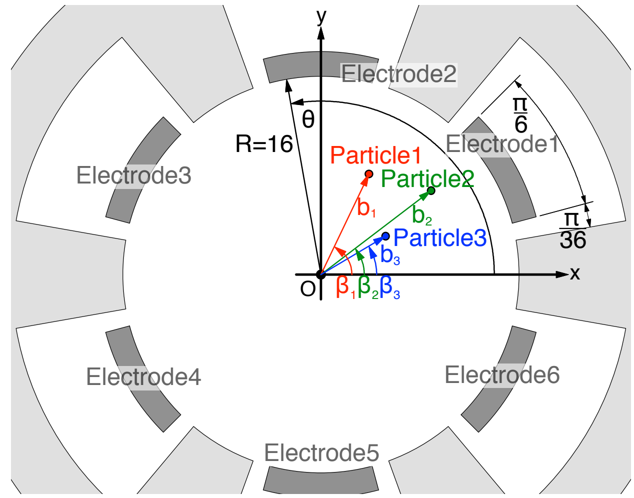

Figure 1: Structure of six-electrode BPM with a typical three-particle system.

Because the electric field on inner surface $E(\theta)$ is a superposition of the electric field generated by all the charged particles, i.e., a beam, $E(\theta)$ is written as follows in Eq. (1) [1]:

$$
\begin{aligned}
E(\theta) &\propto M + 2\sum_{n=1}^{\infty}\sum_{N=1}^{M}\frac{p_{Nn}\cos n\theta + q_{Nn}\sin n\theta}{R^n},\\
&\propto 1 + 2\sum_{n=1}^{\infty}\frac{P_n\cos n\theta + Q_n\sin n\theta}{R^n},\\
p_{Nn} &= b_N^n\cos n\beta_N,\ q_{Nn} = b_N^n\sin n\beta_N,\\
P_n &= \frac{1}{M}\sum_{N=1}^{M}p_{Nn},\ Q_n = \frac{1}{M}\sum_{N=1}^{M}q_{Nn}.
\end{aligned}
\tag{1}
$$

In Eq. (1), p_{Nn} and q_{Nn} are the nth-order moments of the Nth-charged particle, and P_n and Q_n are the nth-order absolute moments [1] of the beam.

Output Voltages from Electrode

The output voltage from the dth electrode ($1 \leqq d \leqq 6$) is written as Eq. (2) using geometrical factors c_{dn}, s_{dn}:

$$
\begin{aligned}
V_d &\propto R\int_{(4d-3)\pi/12}^{(4d-1)\pi/12}E(\theta)d\theta = \frac{\pi}{12} + \sum_{n=1}^{\infty}\frac{c_{dn}P_n + s_{dn}Q_n}{R^n},\\
c_{dn} &= \int_{(4d-3)\pi/12}^{(4d-1)\pi/12}\cos n\theta d\theta,\ s_{dn} = \int_{(4d-3)\pi/12}^{(4d-1)\pi/12}\sin n\theta d\theta.
\end{aligned}
\tag{2}
$$

If we treat moments up to the fifth-order, all of the geometrical factors can be summarized as f_n, h_n ($1 \leqq n \leqq 5$) in

* ken@spring8.or.jp

Eq. (3):

$$\begin{aligned}
&f_1 = c_{11} = -c_{31} = -c_{41} = c_{61},\ 0 = c_{21} = c_{51},\\
&h_1 = s_{11} = s_{31} = -s_{41} = -s_{61},\ 2h_1 = s_{21} = -s_{51},\\
&f_2 = c_{12} = c_{32} = c_{42} = c_{62},\ 2f_2 = -c_{22} = -c_{52},\\
&h_2 = s_{12} = -s_{32} = s_{42} = -s_{62},\ 0 = s_{22} = s_{52},\\
&0 = c_{13} = c_{23} = c_{33} = c_{43} = c_{53} = c_{63},\\
&h_3 = s_{13} = -s_{23} = s_{33} = -s_{43} = s_{53} = -s_{63},\\
&f_4 = -c_{14} = -c_{34} = -c_{44} = -c_{64},\ 2f_4 = c_{24} = c_{54},\\
&h_4 = s_{14} = -s_{34} = s_{44} = -s_{64},\ 0 = s_{24} = s_{54},\\
&f_5 = -c_{15} = c_{35} = c_{45} = -c_{65},\ 0 = c_{25} = c_{55},\\
&h_5 = s_{15} = s_{35} = -s_{45} = -s_{65},\ 2h_5 = s_{25} = -s_{55}.
\end{aligned} \tag{3}$$

Differences of Output Voltages

To obtain the beam's nth-order moments, we carefully choose the differences of output voltages C_n, S_n:

$$\begin{aligned}
C_1 &= \frac{V_1 - V_3 - V_4 + V_6}{V_1 + V_3 + V_4 + V_6},\ S_1 = \frac{V_1 + V_3 - V_4 - V_6}{V_1 + V_3 + V_4 + V_6},\\
C_2 &= \frac{V_1 + V_3 + V_4 + V_6 - 2(V_2 + V_5)}{V_1 + V_3 + V_4 + V_6 + 2(V_2 + V_5)},\\
S_2 &= \frac{V_1 - V_3 + V_4 - V_6}{V_1 + V_3 + V_4 + V_6},\ S_3 = \frac{V_1 - V_2 + V_3 - V_4 + V_5 - V_6}{V_1 + V_2 + V_3 + V_4 + V_5 + V_6}.
\end{aligned} \tag{4}$$

Then we suppose that P_n, Q_n can be expressed as a product of an nth power of effective aperture radius R^n_{CnPn}, R^n_{SnQn} [2] and corrected difference $C^\dagger_n, S^\dagger_n$, as shown in Eq. (5):

$$\begin{aligned}
&P_1 = \frac{R_{C1P1}}{2} C^\dagger_1,\ Q_1 = \frac{R_{S1Q1}}{2} S^\dagger_1,\ P_2 = \frac{R^2_{C2P2}}{2} C^\dagger_2,\\
&Q_2 = \frac{R^2_{S2Q2}}{2} S^\dagger_2,\ Q_3 = \frac{R^3_{S3Q3}}{2} S^\dagger_3.
\end{aligned} \tag{5}$$

$$\begin{aligned}
&R_{C1P1} = \frac{\pi}{6f_1} R,\ R_{S1Q1} = \frac{\pi}{6h_1} R,\ R_{C2P2} = \sqrt{\frac{\pi}{9f_2}} R,\\
&R_{S2Q2} = \sqrt{\frac{\pi}{6h_2}} R,\ R_{S3Q3} = \sqrt[3]{\frac{\pi}{6h_3}} R.
\end{aligned} \tag{6}$$

Relations Between $C^\dagger_n$, $S^\dagger_n$ and C_n, S_n

Because V_d is expressed as the linear combination of P_n and Q_n up to the infinite-order (Eq. (2)), we must confine the highest-order of the moments when P_n, Q_n is calculated using the relation of Eq. (5).

If we only confine the fundamental (smallest) order, i.e., without correction, we obtain the following relations between $C^\dagger_n, S^\dagger_n$ and C_n, S_n, as shown in Eq. (7):

$$C^\dagger_1 = C_1,\ S^\dagger_1 = S_1,\ C^\dagger_2 = C_2,\ S^\dagger_2 = S_2,\ S^\dagger_3 = S_3. \tag{7}$$

If we confine the correction with up to third-order moments, we obtain the following recursive relations of Eq. (8):

$$\begin{aligned}
&C^\dagger_1 = C_1 \left(1 + \frac{2P_2}{R^2_{C1P2d}}\right),\ S^\dagger_1 = S_1 \left(1 + \frac{2P_2}{R^2_{S1P2d}}\right) - \frac{2Q_3}{R^3_{S1Q3u}},\\
&C^\dagger_2 = C_2 \left(1 - \frac{2P_2}{R^2_{C2P2d}}\right),\ S^\dagger_2 = S_2 \left(1 + \frac{2P_2}{R^2_{S2P2d}}\right),\ S^\dagger_3 = S_3.
\end{aligned} \tag{8}$$

$$\begin{aligned}
&R_{C1P2d} = \sqrt{\frac{\pi}{6f_2}} R,\ R_{S1P2d} = \sqrt{\frac{\pi}{6f_2}} R,\ R_{S1Q3u} = \sqrt[3]{\frac{\pi}{6h_3}} R,\\
&R_{C2P2d} = \sqrt{\frac{\pi}{3f_2}} R,\ R_{S2P2d} = \sqrt{\frac{\pi}{6f_2}} R.
\end{aligned} \tag{9}$$

If we confine the correction with up to fifth-order moments, we obtain the following recursive relations of Eq. (10):

$$\begin{aligned}
&C^\dagger_1 = C_1 \left(1 + \frac{2P_2}{R^2_{C1P2d}} - \frac{2P_4}{R^4_{C1P4d}}\right) + \frac{2P_5}{R^5_{C1P5u}},\\
&S^\dagger_1 = S_1 \left(1 + \frac{2P_2}{R^2_{S1P2d}} - \frac{2P_4}{R^4_{S1P4d}}\right) - \frac{2Q_3}{R^3_{S1Q3u}} - \frac{2Q_5}{R^5_{S1Q5u}},\\
&C^\dagger_2 = C_2 \left(1 - \frac{2P_2}{R^2_{C2P2d}} + \frac{2P_4}{R^4_{C2P4d}}\right) + \frac{2P_4}{R^4_{C2P4u}},\\
&S^\dagger_2 = S_2 \left(1 + \frac{2P_2}{R^2_{S2P2d}} - \frac{2P_4}{R^4_{S2P4d}}\right) - \frac{2Q_4}{R^4_{S2Q4u}},\ S^\dagger_3 = S_3.
\end{aligned} \tag{10}$$

$$\begin{aligned}
&R_{C1P4d} = \sqrt[4]{\frac{\pi}{6f_4}} R,\ R_{C1P5u} = \sqrt[5]{\frac{\pi}{6f_5}} R,\ R_{S1P4d} = \sqrt[4]{\frac{\pi}{6f_4}} R,\\
&R_{S1Q5u} = \sqrt[5]{\frac{\pi}{6h_5}} R,\ R_{C2P4d} = \sqrt[4]{\frac{\pi}{3f_4}} R,\ R_{C2P4u} = \sqrt[4]{\frac{\pi}{9f_4}} R,\\
&R_{S2P4d} = \sqrt[4]{\frac{\pi}{6f_4}} R,\ R_{S2Q4u} = \sqrt[4]{\frac{\pi}{6h_4}} R.
\end{aligned} \tag{11}$$

SIMULATION

To evaluate the effect of the correction, we calculated vertical position Q_1 by changing sets P_1, Q_1, and P_{g2} in the simulations. We regarded the other higher-order relative moments, Q_{g2}, P_{g3}, Q_{g3}, P_{g4}, Q_{g4}, P_{g5}, and Q_{g5}, as zero because only P_{g2} was widely varied by normal (not skew) quadrupole magnets. Therefore, the higher-order absolute moments were explicitly written as Eq. (12):

$$\begin{aligned}
P_2 &= p_{G2} + P_{g2},\ p_{G2} = P_1^2 - Q_1^2,\ Q_2 = q_{G2} = 2P_1Q_1,\\
P_3 &= p_{G3} + 3p_{G1}P_{g2},\ p_{G3} = P_1^3 - 3P_1Q_1^2,\ p_{G1} = P_1,\\
Q_3 &= q_{G3} + 3q_{G1}P_{g2},\ q_{G3} = 3P_1^2Q_1 - Q_1^3,\ q_{G1} = Q_1,\\
P_4 &= p_{G4} + 6p_{G2}P_{g2},\ p_{G4} = P_1^4 - 6P_1^2Q_1^2 + Q_1^4,\\
Q_4 &= q_{G4} + 6q_{G2}P_{g2},\ q_{G4} = 4P_1^3Q_1 - 4P_1Q_1^3,\\
P_5 &= p_{G5} + 10p_{G3}P_{g2},\ p_{G5} = P_1^5 - 10P_1^3Q_1^2 + 5P_1Q_1^4,\\
Q_5 &= q_{G5} + 10q_{G3}P_{g2},\ q_{G5} = 5P_1^4Q_1 - 10P_1^2Q_1^3 + Q_1^5.
\end{aligned} \tag{12}$$

The ranges of sets P_1, Q_1, and P_{g2} are shown in Eq. (13):

$$\begin{aligned}
&-4 \leqq \text{Set } P_1 \leqq 4 \text{ [mm] by 0.1 mm steps},\\
&-4 \leqq \text{Set } Q_1 \leqq 4 \text{ [mm] by 0.1 mm steps},\\
&\text{Set } P_{g2} = -2, 11 \text{ [mm}^2\text{]}.
\end{aligned} \tag{13}$$

$E(\theta)$ was derived from two-dimensional electrostatic potentials evaluated by applying a method of images with a mirror point charge [1]. For providing P_{g2} to the simulation we assumed an electric quadrupole.

ISBN 978-3-95450-169-4

The simulated correlation plots are shown in Figs. 2, 3, and 4. The abscissa denotes set Q_1, and the ordinate denotes simulated Q_1. These figures only display the negative regions of Q_1 ($-4 \leqq$ set Q_1, simulated $Q_1 \leqq 0$).

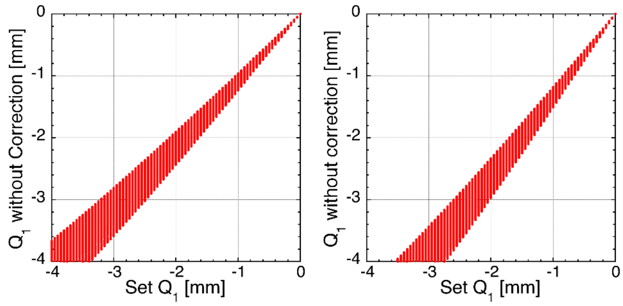

(a) $P_{g2} = -2$ [mm^2] (b) $P_{g2} = 11$ [mm^2]

Figure 2: Simulated Q_1 without correction using Eq. (7).

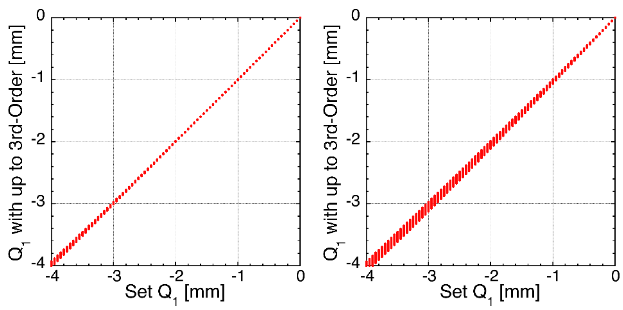

(a) $P_{g2} = -2$ [mm^2] (b) $P_{g2} = 11$ [mm^2]

Figure 3: Simulated Q_1 with up to third-order moment correction using Eq. (8).

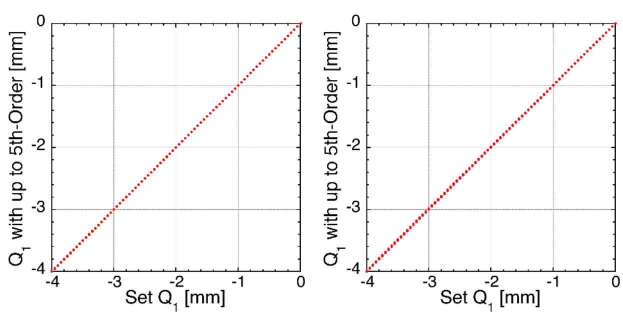

(a) $P_{g2} = -2$ [mm^2] (b) $P_{g2} = 11$ [mm^2]

Figure 4: Simulated Q_1 with up to fifth-order moment correction using Eq. (10).

Small calculation error was shown in the simulated Q_1 with up to fifth-order moment correction (Fig. 4), but huge calculation error was found in the simulated Q_1 without correction (Fig. 2).

COMPARISON WITH EXPERIMENT

To prove the correction's validity, we carried out a beam experiment at SPring-8 linac. The electron beams were swept by horizontal and vertical steering magnets in a $-4 \leqq P_1 \leqq 4$ [mm] and $-4 \leqq Q_1 \leqq 4$ [mm] positional region.

Since we cannot determine the true beam positions, we chose Q_1, which was corrected with up to fifth-order moments instead of set Q_1 as the parameter of abscissa (Figs. 5 and 6).

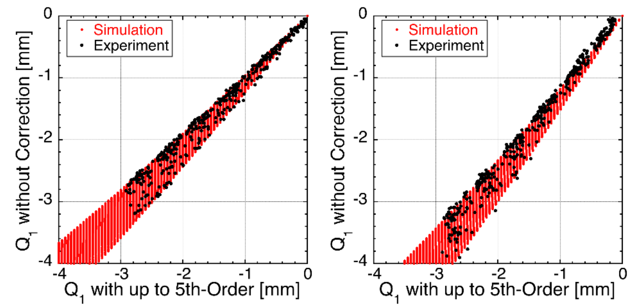

(a) $P_{g2} = -2$ [mm^2] (b) $P_{g2} = 11$ [mm^2]

Figure 5: Correlation plot between Q_1 with up to fifth-order moment correction and Q_1 without it.

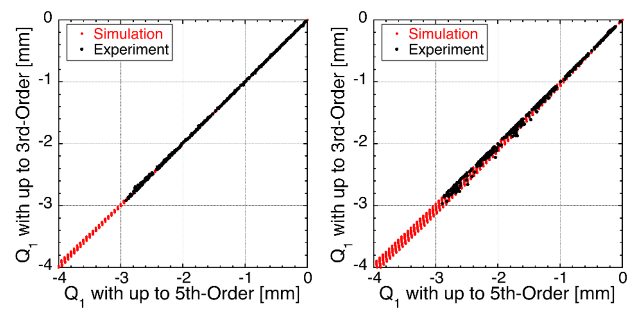

(a) $P_{g2} = -2$ [mm^2] (b) $P_{g2} = 11$ [mm^2]

Figure 6: Correlation plot between Q_1 with up to fifth-order moment correction and Q_1 with up to third-order moment correction.

In the figures, the small red circles (simulation) and the large black circles (experiment) show good agreement, and this consistency proves the validity of higher-order moment correction.

REFERENCES

[1] K. Yanagida *et al.*, *Phys. Rev. ST Accel. Beams* **15**, 012801 (2012).

[2] K. Yanagida *et al.*, "Design and Beam Test of Six-electrode BPMs for Second-Order Moment Measurement," *Proc. of the 26th Int. Linac Conf.*, Tel-Aviv, Sept. 2012, pp. 464-466.

[3] K. Yanagida *et al.*, "Emittance Measurement for SPring-8 Linac Using Four Six-Electrode BPMs," *Proc. of the 27th Int. Linac Conf.*, Geneva, Aug. 2014, pp. 279-281.

[4] K. Satoh and M. Tejima, "Calibration of KEKB Beam Position Monitors," *Proc. of the 19th Particle Accel. Conf.*, Vancouver, May 1997, pp. 2087-2089.